IRAM

300, rue de la Piscine
38406 Saint-Martin-d'Hères (France)
Fax: (33/0) 476 42 54 69

Registration n°: **P294606**
Date: **15-SEP-2016**

PROPOSAL FOR THE 30M TELESCOPE

Title: NIKA2 GT-LP set 1: High-resolution tSZ observations of a large sample of clusters of galaxies (NIKA2SZ)

PIs: Frédéric Mayet (FR), Barbara Comis (FR)
CoIs: Rémi Adam (FR), Peter Ade (GB), Nabila Aghanim (FR), Philippe Andre (FR), Monique Arnaud (FR), Rafael Barrena Delgado (ES) (invited), Iacopo Bartalucci (FR), Alexandre Beelen (FR), Alain Benoit (FR) (invited), Aurelien Bideaud (FR), Nicolas Billot (CH), O. Bourrion (FR), M. Calvo (FR), A. Catalano (FR), Nicolas Clerc (FR), Grégoire Coiffard (IRAMF), Marco De Petris (IT), Francois-Xavier Desert (FR), Marian Douspis (FR), S. Doyle (GB), Chiara Ferrari (FR), J. Goupy (FR) (invited), Carsten Kramer (IRAMS), Samuel Leclercq (IRAMF) (invited), Juan Macias-Perez (FR), P. Mauskopf (GB) (invited), Jean-Baptiste Melin (FR), A. Monfardini (FR), François Pajot (FR), Enzo Pascale (GB), Laurence Perotto (FR), Giampaolo Pisano (GB), Etienne Pointecouteau (FR), Nicolas Ponthieu (FR), Gabriel Pratt (FR), Vincent Reveret (FR), Alessia Ritacco (FR), Louis Rodriguez (FR), Charles Romero (IRAMF), Jose Alberto Rubino Martin (ES), Florian Ruppin (FR), Karl-Friedrich Schuster (IRAMF), Albrecht Sievers (IRAMS), Sebastien Triqueneaux (FR) (invited), C. Tucker (GB) (invited), Robert Zylka (IRAMF), H. Aussel (FR)

Proposal category: Large program
Scientific category: Cosmic Microwave Background (CMB)/Sunyaev-Zel'dovich Effect (SZE), Galaxy Clusters
Observing requirements: pooled

Total requested time: 286.4 (Nika2)

Abstract:
The development of precision cosmology with clusters of galaxies requires high angular resolution observations to extend the understanding of galaxy clusters towards high redshift. The NIKA2 camera at the IRAM 30 m telescope is the only instrument currently in operation that is suited for this kind of observations, given its resolution, sensitivity and dual-band observation capability. We intend to observe a large sample of clusters of galaxies at high redshift ($0.5 < z < 0.9$), selected from the Planck and ACT catalogs. We have formed a representative cluster sample for redshift evolution and cosmological studies, with a homogeneous coverage in cluster mass as reconstructed from the integrated Compton parameter. We will use the SZ-dedicated pipeline that we have developed for the SZ observation with the NIKA camera. Our primary objective is to produce unprecedented high-quality deliverables (tSZ maps and pressure profiles) for all clusters of the sample. NIKA2 data will be complemented with ancillary data including X-ray, optical and radio observations. The full dataset will lead to significant improvements on the use of clusters of galaxies to draw cosmological constraints.

Sources:

Id	Epoch	RA	DEC	z (redshift)
ACT-CL-J0219.8+0022	J2000	02:19:48.792	00:22:31.800	0.537

Id	Epoch	RA	DEC	z (redshift)
ACT-CL-J2152.9-0114	J2000	21:52:56.999	-01:14:44.880	0.69
ACT-CL-J0240.0+0116	J2000	02:40:02.448	01:16:09.480	0.62
ACT-CL-J2302.5+0002	J2000	23:02:34.248	00:02:30.840	0.52
ACT-CL-J0223.1-0056	J2000	02:23:10.536	-00:56:47.760	0.663
PSZ2-G081.02+50.57	J2000	15:39:13.972	50:36:49.474	0.501
PSZ2-G106.15+25.75	J2000	18:57:10.151	74:55:51.105	0.588
PSZ2-G108.27+48.66	J2000	14:27:06.564	65:39:10.113	0.673
PSZ2-G133.59+50.68	J2000	11:46:48.953	65:05:20.718	0.529
PSZ2-G080.64+64.31	J2000	14:27:19.514	44:07:50.915	0.502
PSZ2-G212.44+63.19	J2000	10:52:52.412	24:13:45.938	0.542
PSZ2-G094.56+51.03	J2000	15:08:14.725	57:53:30.411	0.539
PSZ2-G193.31-46.13	J2000	03:35:55.086	-06:59:23.814	0.64
PSZ2-G046.13+30.72	J2000	17:17:07.455	24:03:52.443	0.569
PSZ2-G099.86+58.45	J2000	14:14:42.772	54:47:00.863	0.615
PSZ2-G183.90+42.99	J2000	09:10:47.119	38:48:40.496	0.559
PSZ2-G211.21+38.66	J2000	09:11:13.074	17:48:09.878	0.505
PSZ2-G045.32-38.46	J2000	21:29:25.063	-07:42:32.117	0.594
PSZ2-G144.83+25.11	J2000	06:47:50.958	70:15:26.422	0.584
PSZ2-G201.50-27.31	J2000	04:54:14.205	-03:01:08.475	0.538
PSZ2-G155.27-68.42	J2000	01:37:20.100	-08:28:53.502	0.567
PSZ2-G111.61-45.71	J2000	00:18:34.768	16:26:00.162	0.546
PSZ2-G228.16+75.20	J2000	11:49:36.770	22:24:22.816	0.545
PSZ2-G209.79+10.23	J2000	07:22:23.123	07:24:30.899	0.677
ACT-CL-J0018.2-0022	J2000	00:18:14.952	-00:22:46.200	0.75
ACT-CL-J0058.0+0030	J2000	00:58:04.536	00:30:38.160	0.76
ACT-CL-J2130.1+0045	J2000	21:30:08.810	00:45:32.400	0.71
ACT-CL-J0119.9+0055	J2000	01:19:59.304	00:55:09.480	0.72
ACT-CL-J0215.4+0030	J2000	02:15:28.776	00:30:32.760	0.865
PSZ2-G104.74+40.42	J2000	15:46:50.303	69:56:38.813	0.835
PLCK-G079.95+46.96	J2000	16:02:19.314	51:03:06.534	0.79
PSZ2-G088.98+55.07	J2000	14:59:07.351	52:48:07.289	0.754
PSZ2-G087.39+50.92	J2000	15:26:16.562	54:08:35.067	0.748
PSZ2-G097.52+51.70	J2000	14:55:15.883	58:52:30.865	0.7
PSZ2-G084.10+58.72	J2000	14:49:15.803	48:33:32.215	0.731
PSZ2-G086.93+53.18	J2000	15:13:54.896	52:47:54.298	0.771
PSZ2-G160.83+81.66	J2000	12:26:54.001	33:34:13.180	0.888
PSZ1-G226.65+28.43	J2000	08:56:31.528	01:48:09.104	0.724

Id	Epoch	RA	DEC	z (redshift)
PLCK-G227.99+38.11	J2000	09:32:12.296	05:44:21.723	0.81
PSZ2-G091.83+26.11	J2000	18:31:08.047	62:14:53.134	0.816
PSZ1-G140.10+50.09	J2000	11:10:48.228	63:32:49.231	0.772
PSZ1-G224.73+33.65	J2000	09:11:30.219	05:48:24.485	0.768
PSZ2-G141.77+14.19	J2000	04:41:07.227	68:11:23.844	0.821
PSZ1-G080.66-57.87	J2000	23:27:33.710	-02:03:41.868	0.705
PSZ2-G138.61-10.84	J2000	02:27:06.838	49:05:10.350	0.702
PSZ2-G071.82-56.55	J2000	23:09:32.752	-04:09:29.995	0.87
PSZ2-G092.69+59.92	J2000	14:26:32.327	51:15:07.526	0.82

Nika2 technical sheet:
Time: 286.40
Observing parameters:

Id	1.3mm flux	1.3mm rms	2mm flux	2mm rms	Band priority	Source type	Map size	PWV	Time	Repetition	Remark
1	0.242	0.085	0.753	0.265	2mm	Extended	104.0	2	21.7	1	ACT-CL J0219.8+0022
2	0.284	0.097	0.884	0.301	2mm	Extended	104.0	2	16.8	1	ACT-CL J2152.9-0114
3	0.287	0.099	0.893	0.309	2mm	Extended	104.0	2	16.0	1	ACT-CL J0240.0+0116
4	0.296	0.106	0.923	0.331	2mm	Extended	104.0	2	13.9	1	ACT-CL J2302.5+0002
5	0.346	0.119	1.077	0.372	2mm	Extended	104.0	2	11.0	1	ACT-CL J0223.1-0056
6	0.364	0.134	1.134	0.417	2mm	Extended	104.0	2	8.8	1	PSZ2 G081.02+50.57
7	0.414	0.148	1.288	0.461	2mm	Extended	104.0	2	7.2	1	PSZ2 G106.15+25.75
8	0.449	0.158	1.399	0.491	2mm	Extended	104.0	2	6.3	1	PSZ2 G108.27+48.66
9	0.414	0.152	1.288	0.472	2mm	Extended	104.0	2	6.8	1	PSZ2 G133.59+50.68
10	0.409	0.152	1.275	0.474	2mm	Extended	104.0	2	6.8	1	PSZ2 G080.64+64.31
11	0.462	0.17	1.439	0.53	2mm	Extended	104.0	2	5.4	1	PSZ2 G212.44+63.19
12	0.479	0.177	1.491	0.551	2mm	Extended	104.0	2	5.0	1	PSZ2 G094.56+51.03
13	0.547	0.197	1.704	0.613	2mm	Extended	104.0	2	4.1	1	PSZ2 G193.31-46.13
14	0.54	0.199	1.681	0.62	2mm	Extended	104.0	2	4.0	1	PSZ2 G046.13+30.72
15	0.603	0.221	1.877	0.687	2mm	Extended	104.0	2	3.2	1	PSZ2 G099.86+58.45
16	0.584	0.219	1.818	0.681	2mm	Extended	104.0	2	3.3	1	PSZ2 G183.90+42.99
17	0.56	0.219	1.744	0.682	2mm	Extended	104.0	2	3.3	1	PSZ2 G211.21+38.66
18	0.67	0.249	2.086	0.777	2mm	Extended	104.0	2	2.5	1	PSZ2 G045.32-38.46
19	0.716	0.272	2.231	0.846	2mm	Extended	104.0	2	2.1	1	PSZ2 G144.83+25.11
20	0.693	0.273	2.159	0.849	2mm	Extended	104.0	2	2.1	1	PSZ2 G201.50-27.31

Id	1.3mm flux	1.3mm rms	2mm flux	2mm rms	Band priority	Source type	Map size	PWV	Time	Repetition	Remark
21	0.771	0.301	2.4	0.938	2mm	Extended	104.0	2	1.7	1	PSZ2 G155.27-68.42
22	0.832	0.33	2.592	1.028	2mm	Extended	104.0	2	1.4	1	PSZ2 G111.61-45.71
23	0.888	0.354	2.766	1.102	2mm	Extended	104.0	2	1.3	1	PSZ2 G228.16+75.20
24	1.042	0.392	3.246	1.221	2mm	Extended	104.0	2	1.0	1	PSZ2 G209.79+10.23
25	0.308	0.104	0.958	0.324	2mm	Extended	104.0	2	14.6	1	ACT-CL J0018.2-0022
26	0.304	0.103	0.946	0.322	2mm	Extended	104.0	2	14.7	1	ACT-CL J2130.1+0045
27	0.319	0.109	0.995	0.339	2mm	Extended	104.0	2	13.3	1	ACT-CL J0119.9+0055
28	0.395	0.133	1.231	0.413	2mm	Extended	104.0	2	9.0	1	ACT-CL J0215.4+0030
29	0.458	0.155	1.427	0.483	2mm	Extended	104.0	2	6.5	1	PSZ2 G104.74+40.42
30	0.497	0.171	1.548	0.531	2mm	Extended	104.0	2	5.4	1	PLCK G079.95+46.96
31	0.49	0.17	1.527	0.528	2mm	Extended	104.0	2	5.5	1	PSZ2 G088.98+55.07
32	0.506	0.176	1.577	0.548	2mm	Extended	104.0	2	5.1	1	PSZ2 G087.39+50.92
33	0.486	0.107	1.514	0.53	2mm	Extended	104.0	2	5.4	1	PSZ2 G097.52+51.70
34	0.523	0.183	1.63	0.57	2mm	Extended	104.0	2	4.7	1	PSZ2 G084.10+58.72
35	0.562	0.195	1.749	0.607	2mm	Extended	104.0	2	4.1	1	PSZ2 G086.93+53.18
36	0.646	0.221	2.013	0.688	2mm	Extended	104.0	2	3.2	1	PSZ2 G160.83+81.66
37	0.559	0.197	1.742	0.612	2mm	Extended	104.0	2	4.1	1	PSZ1 G226.65+28.43
38	0.654	0.227	2.036	0.706	2mm	Extended	104.0	2	3.1	1	PLCK G227.99+38.11
39	0.805	0.283	2.507	0.882	2mm	Extended	104.0	2	2.0	1	PSZ2 G091.83+26.11
40	0.775	0.275	2.413	0.855	2mm	Extended	104.0	2	2.1	1	PSZ1 G140.10+50.09
41	0.783	0.278	2.437	0.865	2mm	Extended	104.0	2	2.0	1	PSZ1 G224.73+33.65

Id	1.3mm flux	1.3mm rms	2mm flux	2mm rms	Band priority	Source type	Map size	PWV	Time	Repetition	Remark
42	0.836	0.294	2.605	0.916	2mm	Extended	104.0	2	1.8	1	PSZ2 G141.77+14.19
43	0.814	0.295	2.535	0.92	2mm	Extended	104.0	2	1.8	1	PSZ1 G080.66-57.87
44	0.936	0.344	2.915	1.071	2mm	Extended	104.0	2	1.3	1	PSZ2 G138.61-10.84
45	0.686	0.236	2.136	0.734	2mm	Extended	104.0	2	2.8	1	PSZ2 G071.82-56.55
46	0.582	0.2	1.812	0.624	2mm	Extended	104.0	2	3.9	1	PSZ2 G092.69+59.92
47	0.311	0.105	0.97	0.327	2mm	Extended	104.0	2	14.3	1	ACT-CL J0058.0+0030

Guaranteed time: Yes

Scheduling constraints:
Note that the order of the sources does not reflect the priority order.

High-resolution tSZ observations of a large sample of clusters of galaxies

P.I.: Frédéric Mayet & Barbara Comis (LPSC Grenoble)

1 Scientific Rationale

As the largest gravitationally bound objects in the Universe, clusters of galaxies represent the last step of the hierarchical process of structure formation. Their abundance in mass and redshift is a powerful cosmological probe, as it is sensitive to the primordial density fluctuations and the expansion history and matter content of the Universe.

In a cluster, most of the baryons are present within a gas that is hot (10^6 - 10^8 K), diffuse and completely ionized. It is referred to as the Intra-Cluster Medium (ICM). Cosmic Microwave Background (CMB) photons may interact, via inverse-Compton scaterring, with the free hot electrons in the ICM, being then shifted to higher energies. This interaction, known as the thermal Sunyaev-Zel'dovich (tSZ) effect, results in a CMB flux decrement (increment) at frequencies below (above) 217 GHz. The tSZ brightness is proportional to the integral of the electronic pressure along the line of sight ($y \propto \int P_e \, dl$). Measuring the distribution of the tSZ signal in clusters directly probes the distribution of thermal pressure within the ICM. Furthermore, the tSZ flux is not affected by redshift cosmic dilution as it is a CMB spectral distortion. Thus, the tSZ effect represents a well-suited observable to detect and study clusters at high redshift ($z > 0.4$), where their number and distribution is the most sensitive to the underlying cosmology [1].

In the last few years, technological progresses have made possible the detection of the tSZ effect routinely. As a consequence, tSZ-selected cluster catalogues containing several thousands of candidates have been produced, at arcmin resolution, by the South Pole Telescope (SPT, FWHM $\sim$ 1.1 arcmin at 150 GHz, [2, 3]), the Atacama Cosmology Telescope (ACT, FWHM $\sim$ 1.4 arcmin at 148 GHz, [4]), and the Planck satellite (FWHM $\sim$ 10 arcmin for tSZ, [5]). However, their relatively limited resolution only enables detailed study of the spatial distribution of the signal for nearby clusters. ICM tSZ flux (Y) provides a powerful tool for cosmological investigation with clusters, as long as we are able to convert them into robust estimates of the cluster total mass (M_{tot}). At present, the systematic uncertainties (*e.g.* astrophysical systematics) affecting the mass-observable scaling relations represent the limit for cluster-derived cosmological constraints [5]. Measurements reaching sub-arcminute angular resolution are thus a mandatory step for precise cluster cosmology, since they will contribute to improve our knowledge of the statistical properties of galaxy cluster structure, by reducing the related uncertainties and biases.

The NIKA2 camera at the IRAM 30 m telescope is the only instrument currently in operation that is suited for this kind of observations and follow-ups, given its resolution, sensitivity and dual-band observation capability. Conducting sub-arcminute tSZ observations of a representative population of clusters across the almost unexplored redshift range $0.5 \lesssim z \lesssim 0.9$ will bring detailed insight of the properties of clusters over more than 3 Gyr. This will allow us to understand the processes driving the physical evolution of massive halos in the Universe and to quantify how the cluster thermal content and distribution evolves as massive halos grow through accretion and merging processes. This will result in a better characterization of the mass-observable scaling relations and its potential redshift evolution within a range relevant for the precision of cluster-based cosmological studies. In short, the proposed LP sample will enable a major breakthrough in the use of clusters of galaxies for cosmological studies.

2 Immediate Objective

The main objective of this program is to obtain **high resolution** tSZ observations for a sample of objects, which are **representative** of the population of clusters of galaxies, at **intermediate and high redshifts (z > 0.5)** and spanning one order of magnitude in SZ signal and mass. These observations will be used for an in-depth study of the evolution of cluster physical properties across cosmic times. At present, cluster and tSZ derived cosmological constraints are limited by our incomplete understanding of the impact of the details of cluster astrophysics. Thus, this study is mandatory to handle systematics and achieve precision cosmology with clusters.

Our first objective is to produce, for the whole selected cluster sample, unprecendented high-quality deliverables, such as tSZ maps and pressure profiles (see. Fig. 1), which we will release to the cosmology and astrophysics communities. Then, we will characterize statistically the properties of this high-redshift cluster population, by:

i) Exploring and test the regularity of the cluster pressure profile at $z > 0.5$, following the approach that has been used in X-rays with the REXCESS sample at $z < 0.2$ [6], but with an observable (the SZ signal) that probes directly

the ICM pressure. The major issue is the study of the mass-observable scaling relation and its evolution with the redshift and the cluster dynamical state.

ii) Detecting the presence of sub-structures (*e.g.* secondary peaks, deviations from spherical symmetry, overall irregular shape), their significance and impact on the global Y estimate.

iii) Introducing, defining and testing parameters that allow us to quantify the cluster dynamical state through its tSZ morphology and fluctuations [12]. A robust tSZ-defined indicator of cluster morphology would permit to study the disturbed cluster fraction as a function of redshift and would represent a useful tool to explore its correlation with deviation from the cluster self-similar behavior observed at low z and in hydrodynamical simulations for both the pressure profile and scaling laws, so linking the deviation from the mean to the (thermo-)dynamical history.

iv) Studying the correlation between the SZ indicator(s) of cluster dynamical state, the dispersion around the average cluster pressure profile and its evolution with redshift and radial scale.

This information is essential for understanding cluster formation physics and performing precise cosmological analysis with the cluster population. Of particular importance is the clarification of the physical origin of the normalisation, scatter and evolution of the scaling relations, particularly the mass- SZ observable relation, rendering their empirical calibration and their ultimate cosmological application more robust. The statistical properties of the pressure profiles, in link with the cluster dynamical states, are also a key element for understanding the selection function of the SZ survey.

3 Feasibility and Technical Justification

The NIKA2 camera represents a technological breakthrough for high-resolution observations of the tSZ effect from cluster of galaxies:

– It *operates simultaneously at two frequency* bands, 150 and 260 GHz, at which tSZ shows up respectively as a negative and a slighlty positive distortion of the CMB spectrum, producing a very distinctive cluster signal on the observed maps. For NIKA2, the main SZ signal is expected at 2 mm, while the 1mm band will be used for atmospheric and point-source removal. With NIKA, we have shown that dual-band observations can be used to remove the atmospheric noise without affecting the signal, see [7, 8, 9, 10, 11]. In addition they are of the outmost interest to detect foreground contaminating sources, and account for their flux.

– NIKA2 is made of *arrays of thousands of high sensitive* Kinetic Inductance Detectors (*KIDs*). In particular we expect a sensitivity in Compton parameter units of $\sim 10^{-4}$ per hour and per beam. This should allow us to obtain reliable tSZ detections and mapping of clusters of galaxies in few hours.

– NIKA2, *coupled to the IRAM 30 m telescope* allows us to map clusters of galaxies to a *resolution of typically* 20 arcsec *within a* 6.5 arcmin *diameter FOV*.

NIKA2 tSZ capabilities have been demonstrated through a pilot study conducted with its pathfinder, NIKA. In order to validate the KIDs capabilities when dealing with such a faint and diffuse signal, we have mapped the tSZ in the direction of six clusters of galaxies: **i)** RX J1347.5-1145, an intermediate redshift object ($z = 0.45$), which has been the perfect target for the first tSZ detection ever achieved with KIDs [7]; **ii)** CL J1226.9+3332, a very high redshift cluster, $z = 0.89$ [8], **iii)** MACS J0717.5+3745, which has been used to report the first model-independent mapping of the kinetic Sunyaev-Zel'dovich [9]; **iv)** MACS J1423.9+2404, a relaxed cluster, which has been used to explore the impact of the presence of foreground radio and IR sources and how to deal with them in the data reduction [10]; **v)** PSZ1 G046.13+30.75 and PSZ1 G045.85+57.71, two Planck-discovered clusters (at $z = 0.57$ and $z = 0.61$, respectively) chosen to test NIKA2 capabilities at the level of detection of the Planck catalogue of tSZ sources [11]. We have successfully explored a wide range of cluster morphologies and amplitudes of the tSZ flux.
The MUSTANG and Bolocam instruments (at the focus of the Green Bank Telescope and of the Caltech Submillimeter Observatory, respectively) have also produced high quality tSZ observations. They are expected to be followed by next generation instruments. MUSTANG-2 represents the closest NIKA2 concurrent instrument, even if it will not dispose of simultaneous dual-band capability, together with the next instrument on the LMT (BolocamII, TOLTEC), that will not be ready before NIKA2. As an alternative to large diameter telescopes, interferometers can reach very high angular resolution, but they cannot recover the large scale signal and they are time expensive (see Kitayama 2016 and Basu 2016).

Target selection – Our target selection strategy is mainly driven by the need of selecting **a sample of objects that is representative of the cluster population**. A representative sample, *i.e.* which is not biased towards a given cluster morphology, will allow us *to derive mass-observable scaling relations that can be applicable to the whole cluster*

population (not only relaxed or unrelaxed ICM) and *to achieve a global characterization of clusters and an improved control of systematics due to their astrophysics*. A flux-selected subset of a tSZ-selected cluster catalogue fulfills the requirement of a representative sample. This criterion follows the approach adopted to build the REXCESS sample, an XMM-Newton large program dedicated to the in-depth study of a representative sample of 33 X-ray selected clusters ($0.055 < z < 0.183$). This sample has been used to build the universal pressure profile for the ICM [6], an average profile for the cluster population, derived from observations, scaled by mass and redshift according to the standard self-similar model. The LP SZ sample can be used to continue the characterisation of the cluster statistical properties, further pushing the assessment of the potential evolution of the pressure profile to higher redshifts, where X-ray observation becomes time consuming.

In order to fulfill our goal with NIKA2, we consider the following main target selection criteria:

– clusters belonging to tSZ-selected samples (already existing tSZ based cluster samples from Planck and ACT), for which the redshift information is available;

– $0.5 < z < 0.9$, to explore the cluster statistical properties beyond the local Universe;

– dec > -11, to ensure observability of the sources from the Pico Veleta site.

We have used the above criteria and the Planck and ACT cluster samples to select a representative sample of clusters of galaxies suitable for our purposes. We note however that the external validation of the tSZ-discovered-Planck clusters is not yet fully completed. We consider two bins in redshift ($0.5 < z \leq 0.7$ and $0.7 < z \leq 0.9$), and for each of them, we have defined five bins in $E_z^{-2/3} D_A^2 Y_{500}$ (Fig. 1, bottom panel), which is the quantity related to the cluster mass M_{500} through the scaling relation we aim at calibrating (D_A is the angular diameter distance and $E_z = H(z)/H_0$ accounts for the background universe evolution). Within each bin we have selected 5 clusters maximising, when possible, the overlap with the SZ clusters already planned for X-ray follow-ups with XMM-Newton (large programs PI: M. Arnaud). In summary, we have selected 45 out of 50 clusters and the selected sample is listed in Tab. 1. Note that we have added to the sample two extra clusters (backup) at high redshift (see Table 1), to account for the large uncertainties in the definition of the properties of high redshift clusters. For the two largest $E_z^{-2/3} D_A^2 Y_{500}$ bins (massive clusters) at high redshift we have at present only 4 and 1 cluster respectively. So, in agreement with IRAM, the remaining five clusters will be defined within one year from the starting of the large program. For this purpose, we will take advantage of the information provided by current and near-future Planck and ACT follow-up programs, which are expected to populate the $z > 0.6$ region.

Observing strategy and data reduction – Based on the experience with the NIKA camera, we will perform OnTheFly (OTF) scans in right ascension and declination. We will alternate different orientations of the scans (e.g. 0, 45, 90,-45 degrees) and perform scans of 13' × 8'. Hence, more than one third of the observing time will be spent on the core of the signal. This will allow us to properly define the zero level of the final map and measure angular scales structures up to the scan size. To estimate the expected cluster signal in the maps we use the Y_{500} ($Y_{500} = \int_{\Omega_{r_{500}}} y d\Omega$), M_{500} and redshift provided from the latest updated version of Planck and the cluster catalogs. We then consider an universal pressure profile [6] to model the distribution of the signal around the cluster center for each Y_{500}. The required observation time are optimized cluster by cluster, in order to obtain an homogeneous sample in terms of signal to noise at a given characteristic radius θ_{500} (radius at which the cluster mean over density is equal to 500 times the critical density of the Universe). We impose at least a 1-σ measurement of the cluster pressure profile at θ_{500} (see. Fig. 1) for all clusters in the sample. Notice that the θ_{500} is computed from the redshift and the tSZ-derived M_{500} reported in the catalogues, in order to have a homogeneous definition that only depends on the tSZ flux and the cluster distance.

Transforming the above criteria into a rms noise in the map we compute the observing time per cluster using the NIKA2 time estimator provided by IRAM. We consider millimetre weather conditions with 2 mm of PWV, an overhead factor of two, 60 % of valid detectors and a conservative filtering of about 30 % within the cluster characteristic radius. The expected observing time per cluster are presented in Table 1. We also specify that we have used the y to Jy/beam conversion reported in [8]. Roughly speaking we require observing times of about 10 to 20 hours for the faintest clusters and of 1-3 hours for the most massive ones. To provide an example, by re-projecting the Planck flux for the NIKA observed cluster PSZ1 G045.85+57.71, we obtain an expected tSZ peak at ∼2 mJy/beam (consistently with what shown in [11]). And we recall here that, for this cluster, 4.3 hours of observation with the NIKA prototype allowed a map quality comparable to what we require in this program (allowing a non parametric pressure profile deprojection up to θ_{500}, Fig. 1, upper right panel). In the PSZ catalogue, this cluster has close properties to PSZ2 G046.13+30.72, for which we require 4 hours of observation. For the 45 selected clusters we obtain a total observing time of 280 hours. The total time on pms is 287 as it accounts for the two backup clusters

that may replace two clusters of the sample if needed. The remaining 20 hours will be used to accommodate the observations of the lacking five high mass clusters. In the case of improved instrument performance we intend to keep the same number of sources and the same integration time for each of them, in order to extend morphology analysis out to the cluster outskirts. To illustrate, in the case of goal performance and 30% of overhead time (as reached during NIKA observations), the signal to noise will be improved by a factor of about 2.5.

In terms of data reduction we will use the tSZ dedicated pipeline developed for the NIKA experiment. This pipeline has beed intensively tested using the NIKA data and was used for the NIKA SZ publications [7, 8, 9, 10, 11]. Needed improvements and updates will be directly carried out by our team that led the analysis of the NIKA SZ data. NIKA2 will be able to observe simultaneously at two wavelengths allowing for self consistent foreground source subtraction (e.g. [10]). However NOEMA could be eventually used to obtain complementary information in this sense, requiring reasonable observing times.

4 Organizational Issues

Project management – For this project we have gathered a highly experienced team with a large expertise in submillimetre observations, data reduction and tSZ science as well as complementary external observations. A project PI (F. Mayet) and a co-PI (B. Comis) will coordinate the different activities. As an expert of the NIKA2 pipeline, the co-PI is in charge of coordinating the data reduction, according to NIKA2 collaboration rules. The NIKA2SZ team have a long experience of SZ data with NIKA observations, together with external data for joint analysis. For the sake of clarity, the team can be presented in two sub-teams:

- NIKA2SZ analysis team : R. Adam, B. Comis, M. De Petris, J.-F. Macias Perez, F. Mayet, L. Perotto, C. Romero, F. Ruppin. The NIKA2SZ analysis team has developped a SZ pipeline enabling the processing from raw data to SZ maps and pressure profiles (Fig. 1), which are the main deliverables of this LP. It has been tested and optimized on observation with the NIKA intrument, leading to five papers in the recent years [7, 8, 9, 10, 11].

- NIKA2SZ ancillary data team : M. Arnaud, I. Bartalucci, G. Pratt, E. Pointecouteau (XMM group for X-rays), J. A. Rubino Martin, R. Barrena Delgado (GTC team for optical observations) and C. Ferrari (LOFAR team for radio emission). Experts of external data have contributed to the definition of the cluster sample. Furthermore, to maximize the scientific output of the NIKA2SZ, they are participating in the joint analysis with NIKA2 data. Also, follow-ups are being prepared for the near future. Note that this team has contributed to the NIKA SZ papers, proving the added value of external data [7, 8, 9, 10, 11].

Data policy and deliverables– The data and products of the LP will be made publicly available by the NIKA2 collaboration in a dedicated database after the end of the LP observations, following the standard IRAM rules. These products will consist of the raw data, the calibrated map per cluster and associated processing information, and pressure profiles per cluster.

Complementary external data – The scientific output of the NIKA2 LP could be enriched by the use of high quality external data at other wavelengths or with other probes. Other than the use of publicly available data, formal collaborations are being established to collect extra proprietary data. At this regard, XMM data from a companion X-ray follow-up of high-redshift clusters will be used. With NIKA2 the cluster gas will be finally mapped in tSZ with a quality (in terms of sensitivity and angular resolution) comparable to X-ray, even for intermediate and high-redshift clusters. Thus, the natural combination of these two direct observables of the intra-cluster hot gas will allow us to estimate the total masses (under the assumption of hydrostatic equilibrium) as well as a full physical characterization of the (radial) distribution of the cluster thermodynamic properties: not only pressure, but also temperature ($T_e(r) \propto P_e(r)/n_e(r)$) and entropy ($K(r) \propto P_e(r)n_e^{-5/3}$) which are essential to unveil cluster thermodynamic history. Indeed, the tSZ signal directly probes the gas pressure, while X-ray data deliver the gas density squared and temperature. The different dependencies of tSZ and X on the electron density will also provide a powerful probe of gas clumping, and an improved insight on the cluster tridimensional shape.

Furthermore, optical follow-ups could be performed for a large number of the NIKA2 clusters using the GTC (Gran Telescopio Canarias) imaging and spectroscopy facilities. The combination of tSZ and X-ray data to optical/NIR observations of the cluster galaxies will further help to investigate the connection between galaxy properties (luminosity function, SFR, stellar mass) and those of the ICM, and thereby bring constraints on feedback mechanisms at play within clusters. Moreover, weak lensing measurements will provide complementary measurements of the dark matter distribution and total mass of the clusters, in a totally independent way, then affected by different systematics. Optical mass estimate are not based on the same assumptions. The thermodynamical and dynamical properties of the observed clusters will be compared with outputs from numerical simulations such as MUSIC [13].

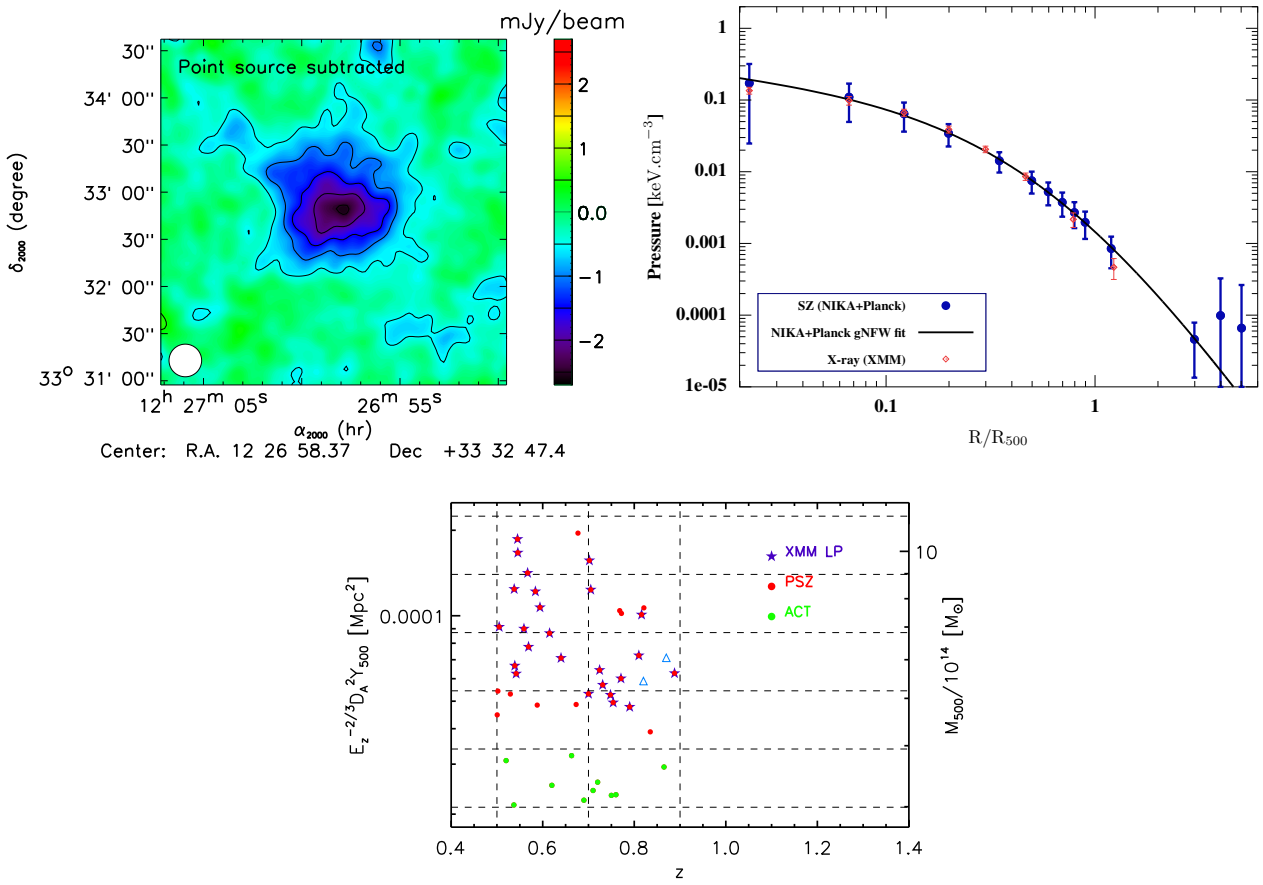

Figure 1: **Upper Left:** NIKA map of CL J1226.9+3332 at 150 GHz [8]. The effective beam FWHM (18.2 arcsec native resolution plus an extra 10 arcsec FWHM Gaussian) is shown as the bottom left white circle. The overall effective observing time on the cluster is 7.8 hours and $\theta_{500} \sim 2$ arcmin for this cluster. **Upper Right:** Non-parametric pressure profile (blue) deprojected from the NIKA tSZ surface brightness map of a Planck-discovered cluster (PSZ1 G045.85+57.71) observed with NIKA in Oct. 2014. Fig. from [11]. This was part of a NIKA pilot study aimed at preparing the NIKA2 tSZ Large Programme. **Bottom** : Clusters extracted from the Planck and ACT (equatorial) tSZ-selected samples, in the redshift range we want to explore and observable from the Pico Veleta site (dec > -11). The different symbol used are reported in the legend, the cyan triangles are the two further objects belonging to the XMM large program (listed at the end of Tab. 1)

References

[1] Carlstrom, J. E., Holder, G. P., & Reese, E. D. 2002, ARA&A, 40, 643

[2] Reichardt, C. L., Stalder, B., Bleem, L. E., et al. 2013, ApJ, 763, 127

[3] Bleem, L. E., Stalder, B., de Haan, T., et al. 2015, ApJS 216, 27

[4] Hasselfield, M., Hilton, M., Marriage, T. A., et al. 2013, J. Cosmology Astropart. Phys., 7, 8

[5] Planck Collaboration, A&A, 571, A29, ArXiv:1502.01598, ArXiv:1502.01597, ArXiv:1502.01596

[6] Arnaud, M., Pratt, G. W., Piffaretti, R., et al. 2010, A&A, 517, A92

[7] Adam, R., Comis, B., Macías-Pérez, J.-F. et al. 2014b, A&A, 569, A66

[8] Adam, R., Comis, B., Macías-Pérez, J.-F. et al. 2015, A&A, 576, A12

[9] Adam, R., Bartalucci, I., Pratt G. W. et al. 2016, ArXiv:1606.07721

[10] Adam, R., Comis, B., Bartalucci, I. et al. 2016, A&A, 586, A122

[11] Ruppin, F., Adam, A., Comis, B., et al. 2016, ArXiv:1607.07679, to appear in A& A

Name	Alternative Name	z	θ_{500} [arcmin]	Y_{500} [10^{-4} arcmin^2]	t_{obs} [hr]
ACT-CL J0219.8+0022		0.537	2.169	1.700	21.7
ACT-CL J2152.9-0114		0.690	1.820	1.500	16.9
ACT-CL J0240.0+0116		0.620	2.022	1.800	16.0
ACT-CL J2302.5+0002		0.520	2.381	2.500	13.9
ACT-CL J0223.1-0056		0.663	2.023	2.200	11.0
PSZ2 G081.02+50.57	RMJ153906.4+503644.9	0.501	2.650	3.739	8.8
PSZ2 G106.15+25.75	PSZ1 G106.15+25.76	0.588	2.396	3.573	7.2
PSZ2 G108.27+48.66	PSZ1 G108.26+48.66	0.673	2.185	3.304	6.3
PSZ2 G133.59+50.68	RMJ114649.1+650506.8	0.529	2.626	4.228	6.8
PSZ2 G080.64+64.31	RMJ142716.1+440730.6	0.502	2.741	4.523	6.8
PSZ2 G212.44+63.19	PSZ1 G212.51+63.18, RMJ105252.4+241530.0, WHL J163.208+24.18	0.542	2.663	4.896	5.4
PSZ2 G094.56+51.03	PSZ1 G094.54+51.01, RMJ150822.0+575515.2, WHL J227.050+57.90	0.539	2.706	5.244	5.0
PSZ2 G193.31-46.13	PSZ1 G193.29-46.13, PLCK G193.3-46.1	0.640	2.426	4.957	4.0
PSZ2 G046.13+30.72	PSZ1 G046.13+30.75, RMJ171705.5+240423.6	0.569	2.679	5.868	4.0
PSZ2 G099.86+58.45	PSZ1 G099.84+58.45, WHL J213.697+54.78	0.615	2.589	6.213	3.2
PSZ2 G183.90+42.99	PSZ1 G183.92+42.99, RMJ091051.0+385022.4, WHL J137.713+38.83	0.559	2.788	6.884	3.3
PSZ2 G211.21+38.66	PSZ1 G211.23+38.63, RXC J0911.1+1746, RMJ091111.5+174628.9	0.505	3.008	7.575	3.3
PSZ2 G045.32-38.46	MACSJ2129.4-0741, RMJ212926.1-074127.9, J2129.4-0741	0.594	2.758	7.841	2.5
PSZ2 G144.83+25.11	PSZ1 G144.86+25.09, MACSJ0647.7+7015, RXC J0647.8+7014	0.584	2.859	9.026	2.0
PSZ2 G201.50-27.31	PSZ1 G201.50-27.34, MACSJ0454.1-0300, RXC J0454.1-0300	0.538	3.043	9.783	2.1
PSZ2 G155.27-68.42	PSZ1 G155.25-68.42, RMJ013725.0-082722.7, WHL J24.3324-8.477	0.567	3.002	10.711	1.7
PSZ2 G111.61-45.71	PSZ1 G111.60-45.72, RXC J0018.5+1626, CL 0016+1609	0.546	3.182	12.991	1.4
PSZ2 G228.16+75.20	PSZ1 G228.21+75.20, RXC J1149.5+2224, RMJ114935.7+222354.6, MCS J1149.5+2223	0.545	3.250	14.522	1.3
PSZ2 G209.79+10.23	PSZ1 G209.80+10.23	0.677	2.819	13.220	1.0
ACT-CL J0018.2-0022		0.750	1.739	1.500	14.6
ACT-CL J0058.0+0030		0.760	1.742	1.500	14.3
ACT-CL J2130.1+0045		0.710	1.823	1.600	14.7
ACT-CL J0119.9+0055		0.720	1.825	1.700	13.3
ACT-CL J0215.4+0030		0.865	1.648	1.800	9.0
PSZ2 G104.74+40.42	PSZ1 G104.78+40.45	0.835	1.816	2.417	6.5
PLCK G079.95+46.96		0.790	1.955	3.013	5.4
PSZ2 G088.98+55.07	PSZ1 G089.04+55.07	0.754	2.029	3.178	5.5
PSZ2 G087.39+50.s92	PSZ1 G087.32+50.92, AMF J231.538+54.13	0.748	2.064	3.393	5.0
PSZ2 G097.52+51.70		0.700	2.162	3.530	5.4
PSZ2 G084.10+58.72	PSZ1 G084.04+58.75	0.731	2.128	3.717	4.7
PSZ2 G086.93+53.18	PSZ1 G086.93+53.18, WHL J228.466+52.83	0.771	2.074	3.828	4.1
PSZ2 G160.83+81.66	BVH2007 154, CL J1226.9+3332	0.888	1.907	3.827	3.2
PSZ1 G226.65+28.43	WHL J134.086+1.780	0.724	2.190	4.209	4.0
PLCK G227.99+38.11		0.810	2.079	4.532	3.1
PSZ2 G091.83+26.11	PSZ1 G091.82+26.11	0.816	2.200	6.298	2.0
PSZ1 G140.10+50.09		0.772	2.286	6.486	2.1
PSZ1 G224.73+33.65	CXOMP J091126.6+05	0.768	2.303	6.647	2.0
PSZ2 G141.77+14.19	PSZ1 G141.73+14.22, WHT	0.821	2.214	6.641	1.8
PSZ1 G080.66-57.87	ACT-CL J2327.4-0204	0.705	2.518	8.182	1.8
PSZ2 G138.61-10.84	PSZ1 G138.60-10.85	0.702	2.639	10.395	1.3
PSZ2 G071.82-56.55	*MEGACAM (redshift id)*	*0.870*	*1.978*	*4.358*	*2.8*
PSZ2 G092.69+59.92	*MEGACAM (redshift id)*	*0.820*	*1.984*	*3.669*	*3.9*

Table 1: Clusters selected for the NIKA2 SZ large program. We report the Planck/ACT name of the object, the alternative names, the redshift, θ_{500}, Y_{500} and the estimated time. In italics, we list two backup objects from the XMM large program.

[12] R. Khatri and M. Gaspari, arXiv:1604.03106

[13] F. Sembolini, M. De Petris, G. Yepes, *et al.* (2014), MNRAS, **440**, 3520